RSC Advances

PAPER

View Article Online
View Journal | View Issue

Cite this: *RSC Adv.*, 2017, **7**, 4196

Luminescent properties of benzothiazole derivatives and their application in white light emission

Fengxian Lu, Rui Hu,* Shuangqing Wang, Xudong Guo and Guoqiang Yang*

Received 17th October 2016
Accepted 5th December 2016

DOI: 10.1039/c6ra25369e

www.rsc.org/advances

Three benzothiazole derivatives, *N*-[4-(benzothiazol-2-yl)-3-hydroxyphenyl]-octanamide (BHPO1), *N*-[3-(benzothiazol-2-yl)-4-hydroxyphenyl]-octanamide (BHPO2), *N*-[4-(benzothiazol-2-yl)phenyl]-octanamide (BPO) were prepared and their luminescence properties were investigated. These analogues show similar absorption maxima but quite different emission regions due to the existence of an excited-state intramolecular proton transfer (ESIPT) process in BHPO1 and BHPO2. Upon excitation with 365 nm light, BPO, BHPO1 and BHPO2 exhibit bright blue-violet, green and orange emission in aggregated states, respectively which perfectly make up the component elements of white light. By doping these compounds into a polymer matrix at a certain proportion, an emission that lies at the saturated white-light region with CIE chromaticity coordinates of (0.31, 0.32) was obtained. This study provides a flexible and simple fabrication process of a white-light emitting device using three structurally-similar compounds without detrimental energy transfer.

1 Introduction

During the past decade, white organic light-emitting diodes (WOLED) and polymer white light-emitting diodes (PWLED) have garnered much attention due to their great potential applications in full-color flat-panel electroluminescent (EL) displays, back-lighting sources for liquid-crystal displays and next-generation solid-state lighting sources.[1–4] Two approaches have been used to obtain a white LED. One is the combination of two or three LEDs with proper power and color ratios, and the other is using a blue or an ultraviolet LED coated with a single phosphor or a mixture of phosphors. All these strategies show some disadvantages. The different lifetimes of LEDs in the former strategy may cause changes in emission color over time. LEDs coated with a single phosphor may suffer a poor color rendition, and LEDs coated with a mixture of phosphors may encounter not only the poor color rendition but also efficiency losses caused by energy transfer between the phosphors.[5–7] Considerable efforts have been devoted to developing phosphor sources with emission over the whole visible range. Among them, mixing multiple chromophores in a suitable host is a relatively simple and cost-effective approach. However, this approach generally requires partial energy transfer from a wide band-gap donor to a narrower band-gap acceptor, and thus results in a trade-off problem between efficiency and color which is rather difficult to balance.[8] Furthermore, white light emitters based on energy transfer processes are always sensitive to the concentration and miscibility of components in matrix, which make it difficult to finely control and reproduce the color.[9–11]

In order to overcome the drawbacks of the above multi-component white light emitters, several research groups have developed some methods and technologies, which include use of hybrid lanthanide organic complexes,[12–14] excimer/exciplex approach,[15–18] interligand energy transfer (ILET),[19] and excited-state intramolecular proton transfer (ESIPT) systems.[20–23] ESIPT compounds display an abnormally large stokes shift without self-absorption due to their unique four-level photophysical cycle process after photoexcitation, which exhibit high photostability and become a kind of potential illuminant materials.[24,25] 2-(2′-Hydroxyphenyl)benzothiazol (HBT) is a typical ESIPT group, which exhibits an environmental-sensitive dual-mode fluorescence,[26] a higher energy enol tautomer emission in protic solvent and a lower energy keto tautomer emission in aprotic environment and solid states.

In the present work, three analogues of benzothiazole derivatives were designed and synthesized. *N*-[4-(Benzothiazol-2-yl)-3-hydroxyphenyl]-octanamide (BHPO1) and *N*-[3-(benzothiazol-2-yl)-4-hydroxyphenyl]-octanamide (BHPO2) are ESIPT compounds, and *N*-[4-(benzothiazol-2-yl)phenyl]-octanamide (BPO) is designed without ESIPT process. The terminal alkyl long chain was incorporated in order to improve the solubility, miscibility and film forming properties of these resultants. Due to the existence of ESIPT process, BHPO1 and BHPO2 exhibit bright green and orange emission in solid state,

Beijing National Laboratory for Molecular Sciences, Key Laboratory of Photochemistry, Institute of Chemistry, University of Chinese Academy of Sciences, Chinese Academy of Sciences, Beijing 100190, China. E-mail: hurui@iccas.ac.cn; gqyang@iccas.ac.cn; Fax: +86-10-82617315; Tel: +86-10-82617263

respectively, with obvious aggregation-induced enhanced emission (AIEE) phenomena while BPO shows a blue-violet emission both in its monodispersed and solid state. Little overlap between the absorptions and emissions can be observed indicating that energy transfer process among these compounds scarcely occurs and the individual emission of each compound can be well maintained while concurrently exciting the mixture of the three compounds. By dispersing the three benzothiazole derivatives into solid polymer matrix with a certain proportion, a saturated white-light emission with Commission Internationale de L'Eclairage (CIE) coordinates of (0.31, 0.32) under 365 nm UV lamp was observed. The three-analogues/polymer system provides a potential color-stable, color-reproducible, and simple-tunable white organic light-emitting source in LED fabrication.

2 Materials and methods

(1) General materials and methods

All the chemicals are commercially available. *n*-Caprylic acid, polyphosphoric acid (PPA) and polymethyl methacrylate (PMMA) were bought from Beijing Chemical Reagents. 1,1′-Carbonyldiimidazole (CDI), 2-aminothiophenol, 4-aminobenzoic acid were purchased from Acros, and 4-aminosalicylic acid, 5-aminosalicylic acid were obtained from Alfa Aesar. All solvents were used after appropriate distillation or purification.

Chemical structures were characterized by ^{1}H-NMR (Bruker, AvanceIII 400), ESI-MS (Waters MicromassQ-TOF) or MALDI-TOF-MS (Bruker BIFLEXIII) and elemental analysis (CarloErba 1106). Absorption spectra were recorded using Hitachi U-3010 spectrophotometer and the fluorescence emission spectra were recorded with a Hitachi F-7000 fluorescence spectrophotometer. Absolute fluorescence quantum yields were determined with a Hamamatsu Quantaurus-QY C11347-11 Spectrometer. Fluorescence lifetimes were measured with a Hamamatsu Quantaurus-Tau C11367-11 Spectrometer.

(2) Synthesis of BHPO1, BHPO2 and BPO (Scheme 1)

Synthesis of *N*-[4-(benzothiazol-2-yl)-3-hydroxyphenyl]-octanamide (BHPO1). 2-(4-Amino-2-hydroxyphenyl)benzothiazole (AHBA) was synthesized according to the literature.[27] To a solution of *n*-caprylic acid (2.16 g, 15 mmol) in 50 mL toluene was added 1,1′-carbonyldiimidazole (CDI, 2.43 g, 15 mmol) under dry argon. The mixture was stirred at reflux temperature for 6 hours and then cooled down to room temperature. Then AHBA (2.42 g, 10 mmol) was added, and the mixture was allowed to reflux overnight with stirring. After the solvent was evaporated under reduced pressure, the crude product was further purified by silica-gel column chromatography with ethyl acetate/*n*-hexane (1 : 3) as the eluent. ^{1}H-NMR (400 MHz, $CDCl_3$) δ 12.63 (s, 1H), 7.94 (d, J = 8.00 Hz, 1H), 7.88 (d, J = 8.00 Hz, 1H), 7.62 (d, J = 8.40 Hz, 1H), 7.49 (t, J = 7.60 Hz, 1H), 7.39 (t, J = 7.60 Hz, 1H), 7.27 (d, J = 6.80 Hz, 1H), 7.20 (d, J = 6.80 Hz, 2H), 2.38 (t, J = 7.60 Hz, 2H), 1.74 (m, 2H), 1.36–1.29 (m, 8H), 0.88 (t, J = 6.60 Hz, 3H). EI-MS (m/z): $[M]^+$ calcd for $C_{21}H_{24}N_2O_2S$ 368.16, found 368. Anal. calcd for $C_{21}H_{24}N_2O_2S$: C, 68.45; H, 6.56; N, 7.60, found: C, 68.19; H, 6.61; N, 7.43.

Synthesis of *N*-[3-(benzothiazol-2-yl)-4-hydroxyphenyl]-octanamide (BHPO2) and *N*-[4-(benzothiazol-2-yl)phenyl]-octanamide (BPO). BHPO2 and BPO were synthesized following the same procedure as BHPO1 except using 2-(5-amino-2-hydroxyphenyl)benzothiazole and 4-(benzothiazol-2-yl) aniline instead of 2-(4-amino-2-hydroxyphenyl)benzothiazole respectively. BHPO2: ^{1}H-NMR (400 MHz, $CDCl_3$) δ 12.47 (t, J = 16.80 Hz, 1H), 8.13 (d, J = 2.40 Hz, 1H), 7.98 (d, J = 8.40 Hz, 1H), 7.90 (d, J = 8.00 Hz, 1H), 7.49 (t, J = 7.20 Hz, 1H), 7.42 (t, J = 7.60 Hz, 1H), 7.33–7.30 (m, 1H), 7.19 (s, 1H), 7.05 (d, J = 8.80, 1H), 2.38 (t, J = 7.60, 2H), 1.76 (m, 2H), 1.39–1.30 (m, 8H), 0.89 (t, J = 6.80, 3H). EI-MS (m/z): $[M]^+$ calcd for $C_{21}H_{24}N_2O_2S$ 368.16, found 368. Anal. calcd for $C_{21}H_{24}N_2O_2S$: C, 68.45; H, 6.56; N, 7.60, found: C, 68.10; H, 6.54; N, 7.40. BPO: ^{1}H-NMR (400 MHz, d6-DMSO) δ 10.20 (s, 1H), 8.12 (d, J = 7.60 Hz, 1H), 8.02 (m, 3H), 7.80 (d, J = 8.80 Hz, 2H), 7.53 (t, J = 7.60 Hz, 1H), 7.43 (t, J = 7.40 Hz, 1H), 2.35 (t, J = 7.40 Hz, 2H), 1.61 (m, 2H), 1.29 (m, 8H), 0.86 (t, J = 6.80 Hz, 3H). EI-MS (m/z): $[M]^+$ calcd for $C_{21}H_{24}N_2OS$ 352.16, found 352. Anal. calcd for $C_{21}H_{24}N_2OS$: C, 71.55; H, 6.86; N, 7.95, found: C, 71.37; H, 6.70; N, 8.09.

(3) Preparation of nanoparticles

The nanoparticles were prepared by rapidly injecting 100 μL THF solution of BPO, BHPO1 and BHPO2 (10^{-3} mol L^{-1}) respectively into ddH_2O (10 mL) with vigorous stirring for 30 s at ambient temperature. The samples, with final concentrations of 10^{-5} mol L^{-1}, were immediately taken for UV-vis absorption and fluorescence measurements.

(4) Preparation of dyes doped PMMA films

BHPO1/PMMA (1 : 100, w/w) were dissolved in dichloromethane. The resulting solution was applied onto a commercial UV-LED set to form a covered film for light demonstration. As the same procedure, BPO/PMMA (1 : 100, w/w), BHPO2/PMMA (1 : 100, w/w) and BPO/BHPO1/BHPO2/PMMA (185 : 2 : 17 : 20 400, w/w/w/w) were prepared.

3 Results and discussion

As shown in Scheme 1, BPO, BHPO1 and BHPO2 were readily synthesized through condensation of aminobenzoic acid or aminosalicylic acid with aminobenzenethiol followed by amidation with *n*-caprylic acid. These compounds with similar chemical structure composing of a benzothiazole unit and adjacent *N*-phenyloctanamide unit may offer similar performances such as solubility and thermal stabilities.[28] These synthesized compounds are well soluble in common organic solvents such as THF and chloroform, but insoluble in water. BPO has no hydroxyl group, and the functionalized hydroxyl group of BHPO1 and BHPO2 is located at *m*- and *p*-position of the octanamide group, respectively. The hydroxyl group of BHPO1 and BHPO2 can easily form intramolecular hydrogen bond with adjacent N atom upon excitation, consequently, the intramolecular proton transfer process occurs and keto

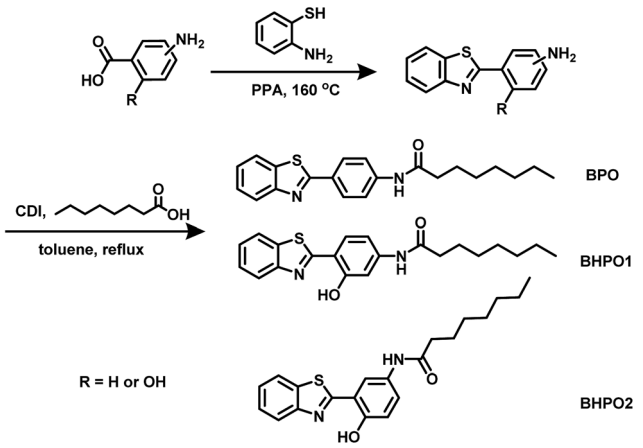

Scheme 1 Structures and synthetic routes of BPO, BHPO1 and BHPO2.

tautomer emission appears in longer wavelength region. The presence of hydroxyl group and the associated hydrogen bond cause essential differences between BPO and BHPO1, BHPO2 in photophysical properties.

The absorption and emission spectra of the solutions of BPO and BHPO1, BHPO2 in THF and the aqueous suspensions of their corresponding nanoparticles are shown in Fig. 1. The absorptions of the three analogues in solution and aggregates almost lie in UV region, indicating that both dilute solution and nanoparticle of these compounds are colorless (Fig. 1a, c and e). Upon excitation with 365 nm light, the solutions of BPO and BHPO1, BHPO2 in THF and the aqueous suspensions of their corresponding nanoparticles show considerable differences in their emission properties. The emission maximum of BPO in THF solution locates at UV region. Due to the enlarged π-electron conjugation in aggregates, the nanoparticle suspension of BPO (BPO/H_2O) exhibits an evident blue-violet emission with a maximum at 425 nm and a fluorescence quantum yield of 0.124 (Fig. 1b). Both BHPO1 and BHPO2 show two emission bands in THF solution (Fig. 1d and f), and the emission bands at the shorter and longer wavelengths are attributed to the enol form and the keto tautomer formed after the ESIPT process, respectively.[29] In the aqueous suspension of BHPO1 and BHPO2, only a ESIPT emission band at longer wavelength is detected, but the emission intensity and lifetime are both enhanced remarkably in aggregates, giving the fluorescence quantum yields of 0.489 (τ = 5.6 ns) and 0.498 (τ = 7.0 ns) for BHPO1 and BHPO2, respectively. The fluorescence enhancement can be ascribed to the so-called AIEE phenomenon. The accepted AIEE mechanism of HBT-type compounds as reported is attributed to the restriction of intramolecular rotation in aggregates, which effectively mitigates the nonradiative decay process and concomitantly enhances the proportion of radiative transitions.[28–31] Although BHPO1 and BHPO2 show similar photophysical characters, the absorption and emission maxima of the corresponding electronic transitions are different. The emission maxima of the keto form for BHPO1 and BHPO2 are 532 and 560 nm (aggregated state), respectively. Evidently, the molecular excited states are modulated by the substituted position of hydroxyl group. The *p*-substituted hydroxyl group contributes more to the electron delocalization of the keto excited state than the *m*-substituted hydroxyl group, resulting in a difference of the stokes shifts, ~170 and ~200 nm for BHPO1 and BHPO2, respectively. As a consequence of the substituted position of hydroxyl group switching from *m*-position to *p*-position, the keto emission shifts from green to orange. Furthermore, the large stokes shifts and the absorption in the UV region of these three compounds can avoid self-absorption and energy transfer between different dyes.

To examine whether BPO, BHPO1 and BHPO2 are suitable to construct multi-component white light emitters, BPO, BHPO1 and BHPO2 are doped into PMMA with a mass fraction of 1%. The normalized fluorescent spectra and corresponding CIE coordinates of PMMA doped with BPO, BHPO1 and BHPO2 are shown in Fig. 2. Emission maximum of dye doped PMMA films is slightly different from their corresponding nanoparticle suspensions, which can be presumably ascribed to the environmental effect. The dye molecules are monodisperse in the dye doped PMMA films, and each dye molecule is surrounded by large amounts of polymer backbone where intermolecular π–π stacking interactions between dye molecules are eliminated. Upon excitation with a 365 nm UV lamp, the emission of BPO, BHPO1 and BHPO2 in PMMA matrix are blue, green and orange, with emission maxima at 398, 528 and 590 nm, respectively. The corresponding CIE coordinates are (0.17, 0.05), (0.28, 0.54), (0.46, 0.52), which constitute a triangle region perfectly covering the white-light equienergy point (0.33, 0.33) in the CIE chromaticity diagram. According to optical principles, the total luminescence color in this triangle region can be easily tuned by blending these three components with precise control of corresponding weight ratios. Moreover, the emissions of these three compounds doped PMMA films are nearly across the entire visible light spectra, giving possibility to produce a pure white light. The absolute fluorescence quantum yields of BPO, BHPO1 and BHPO2 doped PMMA films are measured to be 0.25, 0.30 and 0.22, which are quite receivable. All these photophysical data provide a potential that this set of dye doped PMMA films is used as a kind of white light emitting materials.

The white light emitting material can be fabricated by codoping the three benzothiazole derivatives into PMMA, where determination of the proportion of these three dyes is most pivotal. The binary dye doped PMMA films with different weight ratios of BPO/BHPO1 and BPO/BHPO2 are prepared and studied first to constitute the two edges of the triangle region on the CIE chromaticity diagram. Fig. 3a and b depict the emission spectra changes when tuning the weight ratio of BPO/BHPO1 and BPO/BHPO2 from 5 : 1 to 50 : 1 (5 : 1, 10 : 1, 20 : 1, 30 : 1, 40 : 1, 50 : 1), respectively, with constant weight ratio of [total dye]/PMMA at 1 : 100. As the proportion of BPO increased, the long wavelength emission from BHPO1 or BHPO2 decreases and the short wavelength emission from BPO enhances gradually. Additive mixing of blue-violet and green produces the shades of cyan in optical principles. Mixing BPO (blue-violet) and BHPO1 (green) with weight ratio gradually changed from 5 : 1 to 50 : 1 shifts the CIE coordinates of emission from green

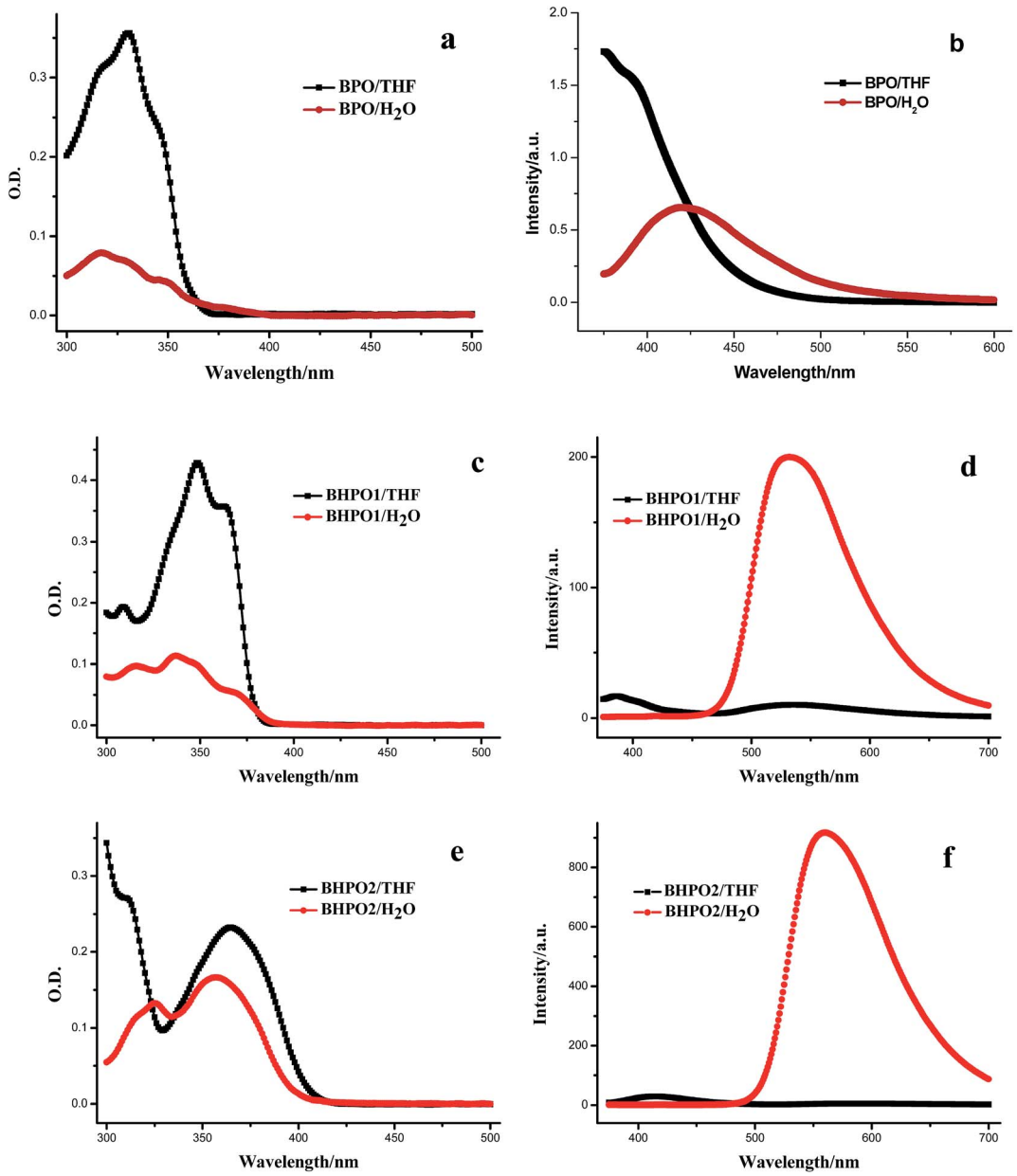

Fig. 1 Absorption and fluorescence spectra of BPO, BHPO1, BHPO2 in THF and water (1.0×10^{-5} mol L^{-1}, $\lambda_{ex} = 365$ nm).

to cyan then to blue-violet region, concomitantly forming the cyan edge of the triangle (Fig. 3c). Representative pictures of films doped with BPO/BHPO1 (0 : 1, 10 : 1, 50 : 1 and 1 : 0, w/w) under excitation are exhibited in Fig. 3d. Similar as BPO/BHPO1 mixtures, the second edge of the triangle from orange to pink then to blue-violet region is subsequently set up by additive mixing of BPO (blue-violet) and BHPO2 (orange) with different weight ratios from 5 : 1 to 50 : 1 (Fig. 3c) and the photos of BPO/BHPO2 (0 : 1, 10 : 1, 20 : 1 and 1 : 0, w/w) doped films under excitation are shown in Fig. 3e.

Following construction of the two edges of the triangle region with binary dye mixtures, hybrid materials with luminescence color over the whitish region can be readily prepared through blending two binary mixtures located on the two edges respectively between which the chord line connected must run through the white light equienergy point. According to this selection rule, BPO/BHPO1 (50 : 1) and BPO/BHPO2 (5 : 1) are perfectly the two mixtures with desirable emission CIE coordinates. Fig. 4a shows the emission spectra of BPO/BHPO1/BHPO2 ternary mixtures through blending BPO/BHPO1 (50 : 1) and BPO/BHPO2 (5 : 1) with weight ratio changing from 4 : 1, 2 : 1, 1 : 1 to 1 : 2 while keeping the weight ratio of [total dye]/PMMA constant (1 : 100, w/w). Increasing the proportion of BPO/BHPO2 (5 : 1) induces the long wavelength emission enhancing as well as broadening gradually. The corresponding CIE coordinates and PMMA film photos of BPO/BHPO1/BHPO2 ternary mixtures are shown in Fig. 4b and c. By fine-tuning the two binary mixtures to 1 : 1, a white light

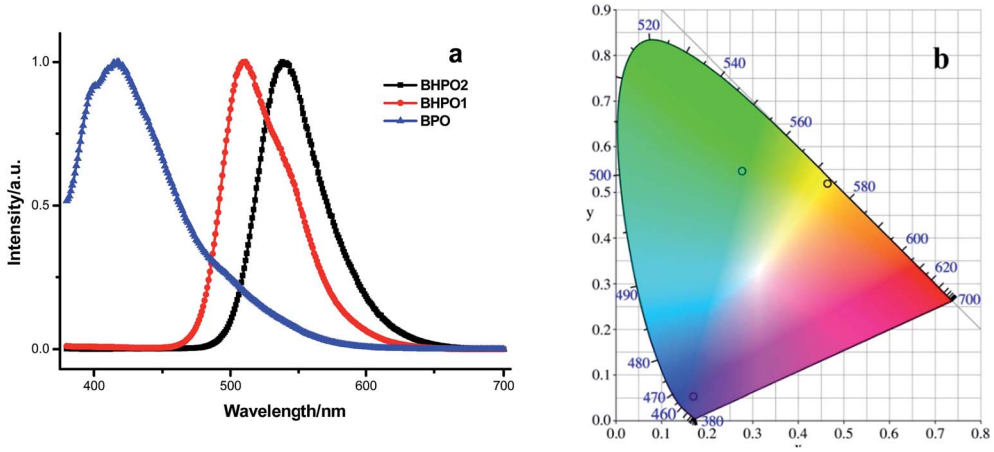

Fig. 2 Fluorescence spectra (a) and the CIE coordinates (b) of BPO, BHPO1, BHPO2 in PMMA film (1 wt%, $\lambda_{ex} = 365$ nm).

emission (0.31, 0.32) is obtained with a weight ratio of BPO/BHPO1/BHPO2 = 185 : 2 : 17.

The dyes/PMMA films, including BPO/PMMA (1 : 100, w/w), BHPO1/PMMA (1 : 100, w/w), BHPO2/PMMA (1 : 100, w/w) and BPO/BHPO1/BHPO2/PMMA (185 : 2 : 17 : 20 400, w/w/w/w), were further applied onto a set of commercial UV-LED (365–375 nm) to form a covered layer. Fig. 4d shows the colorful emissions of UV-LED coated with dye/dyes doped PMMA layers. In the absence of illumination, the appearances of these LEDs are semi-transparent. Upon illumination, blue-violet, green, orange and white light are generated, respectively. The photoluminescent color of these LEDs basically relies on the doped dye components and their corresponding proportions. The emission (0.31, 0.32) of the ternary benzothiazole derivative mixtures with weight ratio of 185 : 2 : 17 (BPO : BHPO1 : BHPO2) in PMMA film is closed to the pure white light

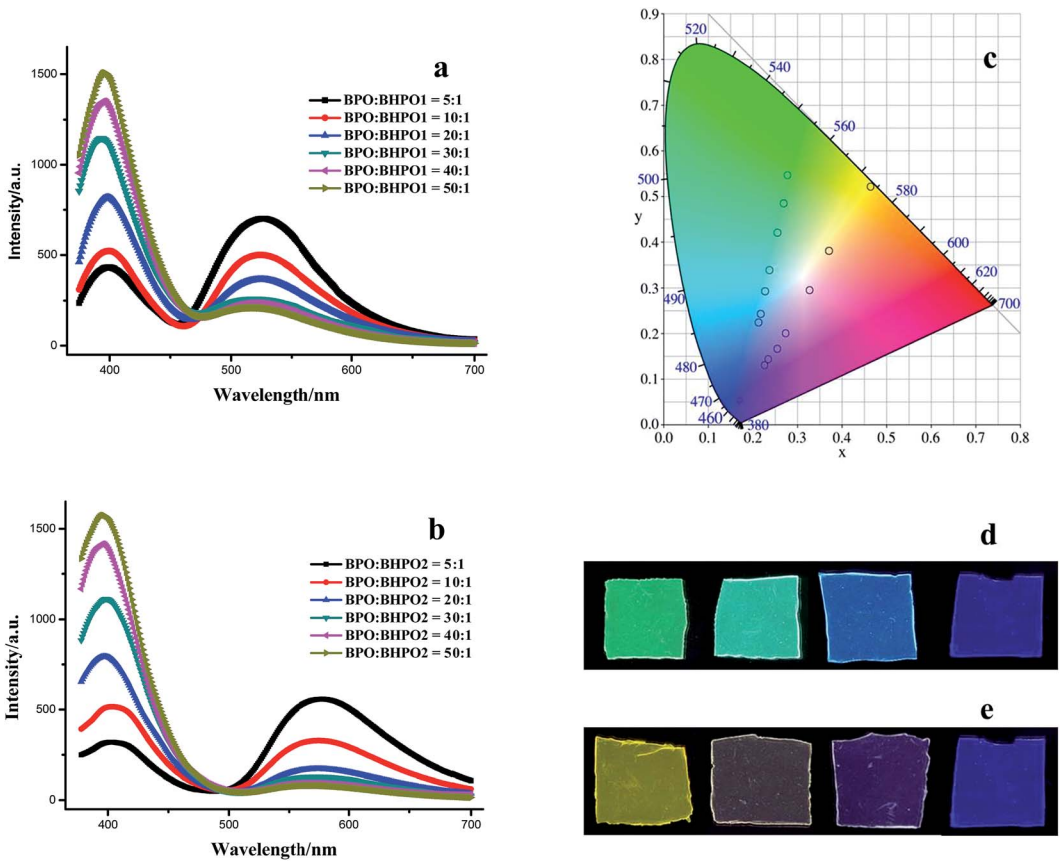

Fig. 3 Fluorescence spectra (a and b), CIE coordinates (c) and the representative pictures (d and e) of binary dye doped PMMA films (the weight ratios of BPO/BHPO1 and BPO/BHPO2 is 5 : 1, 10 : 1, 20 : 1, 30 : 1, 40 : 1, 50 : 1 respectively, w/w).

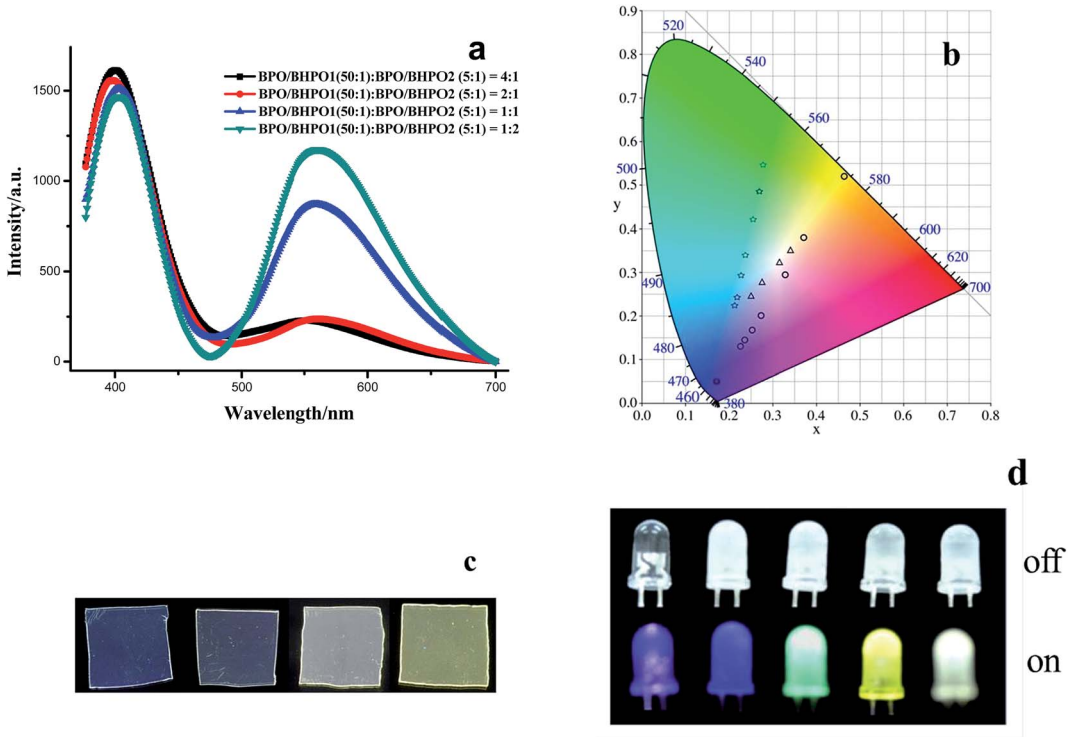

Fig. 4 Emission spectra (a), CIE coordinates (b) and film pictures (c) of the ternary mixtures. Photos of UV LED coated with a thin layer of BPO, BHPO1, BHPO2 and the ternary mixture (185 : 2 : 17, wt%) before and after illumination (d).

(0.33, 0.33), indicating that the mixture of the three benzothiazole homologous analogues can be used as a kind of white organic light-emitting source material.

4 Conclusion

In summary, three benzothiazole derivatives BPO, BHPO1 and BHPO2 were synthesized and their photophysical properties were investigated. All these three analogues show no absorption in the visible region either in homogenous solution or aggregated state. Upon excitation with 365 nm light, BHPO1 and BHPO2 exhibit strong ESIPT emission in aggregated state with large stokes shift. Meanwhile BPO, BHPO1 and BHPO2 doped PMMA films emit violet-blue, green and orange light, respectively, which make up the component elements of white light. By fine-tuning the proportion of these three elements in PMMA matrix, a bright white light with the CIE coordinates of (0.31, 0.32) is easily obtained. This white light generation by mixing homologous ESIPT and non-ESIPT benzothiazole analogues which avoid the detrimental energy transfer between dyes provides a simple approach for preparation of color-tunable light sources.

Acknowledgements

Financial support from the National Basic Research Program of China (2013CB834703, 2013CB834505), the Chinese Academy of Sciences, and the National Natural Science Foundation of China (21233011, 21205122, 21273252 and 21261160488), are gratefully acknowledged. We are also grateful for the assistance of Prof. Yi Li and Dr Yi Zeng from Technical Institute of Physics and Chemistry, Chinese Academy of Sciences.

References

1 Y. R. Sun, N. C. Giebink, H. Kanno, B. W. Ma, M. E. Thompson and S. R. Forrest, *Nature*, 2006, **440**, 908–912.
2 X. Gong, S. Wang, D. Moses, G. C. Bazan and A. J. Heeger, *Adv. Mater.*, 2005, **17**, 2053–2058.
3 Y. Liu, M. Nishiura, Y. Wang and Z. M. Hou, *J. Am. Chem. Soc.*, 2006, **128**, 5592–5593.
4 Q. Wang and D. G. Ma, *Chem. Soc. Rev.*, 2010, **39**, 2387–2398.
5 P. F. Smet, A. B. Parmentier and D. Poelman, *J. Electrochem. Soc.*, 2011, **158**, R37–R54.
6 S. Ye, F. Xiao, Y. X. Pan, Y. Y. Ma and Q. Y. Zhang, *Mater. Sci. Eng., R*, 2010, **71**, 1–34.
7 E. R. Dohner, E. T. Hoke and H. I. Karunadasa, *J. Am. Chem. Soc.*, 2014, **136**, 1718–1721.
8 J. Ye, C. Liu, C. Ou, M. Cai, S. Chen, Q. Wei, W. Li, Y. Qian, L. Xie, B. Mi, Z. Gao and W. Huang, *Adv. Opt. Mater.*, 2014, **2**, 938–944.
9 H. Shono, T. Ohkawa, H. Tomoda, T. Mutai and K. Araki, *ACS Appl. Mater. Interfaces*, 2011, **3**, 654–657.
10 S. Park, J. E. Kwon, S. H. Kim, J. Seo, K. Chung, S.-Y. Park, D. J. Jang, B. M. Medina, J. Gierschner and S. Y. Park, *J. Am. Chem. Soc.*, 2009, **131**, 14043–14049.

11 K. T. Kamtekar, A. P. Monkman and M. R. Bryce, *Adv. Mater.*, 2010, **22**, 572–582.
12 J. Feng and H. J. Zhang, *Chem. Soc. Rev.*, 2013, **42**, 387–410.
13 Y. Liu, L. N. Sun, J. L. Liu, Y. X. Peng, X. Q. Ge, L. Y. Shi and W. Huang, *Dalton Trans.*, 2015, **44**, 237–246.
14 J. H. Liu, X. Q. Ge, L. N. Sun, R. Y. Wei, J. L. Liu and L. Y. Shi, *RSC Adv.*, 2016, **6**, 47427–47433.
15 M. Mazzeo, D. Pisignano, F. Della Sala, J. Thompson, R. I. R. Blyth, G. Gigli, R. Cingolani, G. Sotgiu and G. Barbarella, *Appl. Phys. Lett.*, 2003, **82**, 334–336.
16 J. Karpiuk, E. Karolak and J. Nowacki, *Phys. Chem. Chem. Phys.*, 2010, **12**, 8804–8809.
17 J. Lee, B. Kim, J. E. Kwon, J. Kim, D. Yokoyama, K. Suzuki, H. Nishimura, A. Wakamiya, S. Y. Park and J. Park, *Chem. Commun.*, 2014, **50**, 14145–14148.
18 X. H. Jin, C. Chen, C. X. Ren, L. X. Cai and J. Zhang, *Chem. Commun.*, 2014, **50**, 15878–15881.
19 Y. You, K. S. Kim, T. K. Ahn, D. Kim and S. Y. Park, *J. Phys. Chem. C*, 2007, **111**, 4052–4060.
20 S. Kim, J. Seo, H. K. Jung, J. J. Kim and S. Y. Park, *Adv. Mater.*, 2005, **17**, 2077–2082.
21 W. H. Sun, S. Y. Li, R. Hu, Y. Qian, S. Q. Wang and G. Q. Yang, *J. Phys. Chem. A*, 2009, **113**, 5888–5895.
22 K. I. Sakai, T. Ishikawa and T. Akutagawa, *J. Mater. Chem. C*, 2013, **1**, 7866–7871.
23 K. Benelhadj, W. Muzuzu, J. Massue, P. Retailleau, A. Charaf-Eddin, A. D. Laurent, D. Jacquemin, G. Ulrich and R. Ziessel, *Chem.–Eur. J.*, 2014, **20**, 12843–12857.
24 A. Z. Weller, *Electrochemistry*, 1956, **60**, 1144.
25 P. K. Sengupta and M. Kasha, *Chem. Phys. Lett.*, 1979, **68**, 382–385.
26 Y. Li, Q. Wang, Y. Qian, S. Q. Wang, Y. Li and G. Q. Yang, *J. Phys. Chem. A*, 2007, **111**, 11793–11800.
27 E. Barni, P. Savarino, M. Marzona and M. Piva, *J. Heterocycl. Chem.*, 1983, **20**, 1517–1521.
28 Y. Qian, S. Y. Li, G. Q. Zhang, Q. Wang, S. Q. Wang, H. J. Xu, C. Z. Li, Y. Li and G. Q. Yang, *J. Phys. Chem. B*, 2007, **111**, 5861–5868.
29 R. Hu, S. Y. Li, Y. Zeng, J. P. Chen, S. Q. Wang, Y. Li and G. Q. Yang, *Phys. Chem. Chem. Phys.*, 2011, **13**, 2044–2051.
30 J. E. Kwon and S. Y. Park, *Adv. Mater.*, 2011, **23**, 3615–3642.
31 S. M. Chang, K. L. Hsueh, B. K. Huang, J. H. Wu, C. C. Liao and K. C. Lin, *Surf. Coat. Technol.*, 2006, **200**, 3278–3282.